



Delft University of Technology

Document Version

Accepted author manuscript

Citation (APA)

Ishiyama, T., Ali, M., Blacquiere, G., & Nakayama, S. (2019). Blended acquisition with temporally signed/modulated and spatially dispersed source array. In *SEG Technical Program Expanded Abstracts 2019* (pp. 77-81). Society of Exploration Geophysicists. <https://doi.org/10.1190/segam2019-3214624.1>

Important note

To cite this publication, please use the final published version (if applicable). Please check the document version above.

Copyright

In case the licence states "Dutch Copyright Act (Article 25fa)", this publication was made available Green Open Access via the TU Delft Institutional Repository pursuant to Dutch Copyright Act (Article 25fa, the Taverne amendment). This provision does not affect copyright ownership. Unless copyright is transferred by contract or statute, it remains with the copyright holder.

Sharing and reuse

Other than for strictly personal use, it is not permitted to download, forward or distribute the text or part of it, without the consent of the author(s) and/or copyright holder(s), unless the work is under an open content license such as Creative Commons.

Takedown policy

Please contact us and provide details if you believe this document breaches copyrights. We will remove access to the work immediately and investigate your claim.

This work is downloaded from Delft University of Technology.

Blended acquisition with temporally signatored/modulated and spatially dispersed source array

Tomohide Ishiyama*, ADNOC; Mohammed Ali, Khalifa University; Gerrit Blacquiere, Shotaro Nakayama, Delft University of Technology

Summary

We introduce a blended-acquisition method: temporally signatored and/or modulated and spatially dispersed source array, namely S-/M-DSA. The former S-DSA has much less constraints in the encoding with operational flexibility, allowing non-uniform sampling and non-patterned shooting both in the space and time dimension. The latter M-DSA allows indeed straightforward deblending by filtering and physically separating frequency channels in the frequency domain. We evaluated the deblending performance for several scenarios of blended acquisition. The results showed that: S-DSA attains the best acquisition productivity; M-DSA attains the best deblending performance, compared to other methods. Our S-/M-DSA method makes the blended-acquisition encoding and operations significantly simple and robust; the same is true for the deblending processing.

Introduction

Blended acquisition stands for continuous recording of seismic responses from incoherent shooting, the properties of which are specified by arbitrary spatial and temporal distribution among the sources and their shots involved in the blended-source array (Berkhout, 2008). This acquisition is encoded by the blending operators containing the shot locations, times, signatures, etc. for the blended-source array. There are plenty of examples using some concepts of blended acquisition. Among the various concepts, we come up with a challenging question: what is an optimal blended-acquisition design that is the most suitable for deblended-data-reconstruction processing. In this paper, we introduce a blended-acquisition method: temporally signatored and/or modulated and spatially dispersed source array that can be one of the best blended-acquisition methods.

Method

Blended acquisition is being developed in the industry today in order to alleviate the constraints both in the space and time dimension. In the space dimension, dispersed source array (DSA, Berkhout, 2012; Caporal et al., 2016) is one concept, in which the blended-source array consists of different sources rather than traditional equal ones (e.g. several types of narrow-frequency-banded device instead of a certain type of broad-frequency-banded one). The frequency-banded sources are randomly distributed, and emit the spectrally banded wavefields based on the Nyquist criterion for each frequency band (e.g. optimally coarser sampling for a low frequency source whereas relatively denser sampling for a high frequency one on average). This

allows non-uniform sampling and non-patterned shooting along the space dimension. Furthermore, this yields the frequency-banded wavefields at each shot in the DSA array, thus allows fairly straightforward deblending by filtering naturally in the frequency domain.

Besides, in the time dimension, various signatoring is one concept, in which each shot in the blended-source array is encoded with its own signature, and emits the distinguishable wavefields. This allows non-patterned shooting along the time dimension for each shot in the blended-source array. Furthermore, the signature uniqueness becomes an additional blending property, thus allows more sophisticated deblending by decoding the property, or deconvolving the signature.

Modulation is another concept in the time dimension. Shooting, in particular sweeping for vibrators, is often repeated several times at each shot in order to enhance the S/N. For a shot in the blended-source array, if the sweep wavetrain is exactly repeated, the discrete frequencies, or frequency channels, are made according to the total time length. The sweep wavetrain is allocated at particular frequency channels whereas remaining channels are empty. The empty channels can be assigned for other shots in the blended-source array, in which the sweep wavetrains are modulated along the time dimension, and spectrally shifted in the frequency domain. This is a modulation along the time dimension for each shot in the blended-source array, and does not require complicated signatoring but relatively simple one, in which the instantaneous frequency and amplitude change not quickly but monotonically. Moreover, this allows quite straightforward deblending by physically separating the shot-generated wavefields in the frequency domain.

We introduce a blended-acquisition method using temporally signatored and/or modulated and spatially dispersed source array, namely S-/M-DSA, that jointly uses various signatoring and/or modulation in the time dimension and DSA in the space dimension. S-DSA has much less constraints in the encoding with operational flexibility, allowing non-uniform sampling and non-patterned shooting both in the space and time dimension. M-DSA allows simple and robust deblending by filtering and physically separating frequency channels in the frequency domain.

Examples

The sequent figures illustrate the principle by comparing 3 concepts of blended acquisition: a conventional method, S-

Blended acquisition with S-/M-DSA

DSA and M-DSA. Figure 1 shows the reference data, which is existing real data acquired in Abu Dhabi, and regarded as traditional unblended data, \mathbf{P} . Figures 1a and 1b are without noise attenuation; Figures 1c and 1d are with it. The blended data, \mathbf{P}' , were numerically synthesized with the blending scenarios represented by the blending operators for each case. Those with noise attenuation correspond to noise-attenuated blended data. This is based on the fact that there are several noise-attenuation methods that can be applied to non-uniform and under-sampled blended data beyond aliasing and before deblending (e.g. Ishiyama et al., 2016). Unless otherwise mentioned, the blended data with noise attenuation were used. In the synthesizing process, the number of sources in the blended-source array was 5. The shots were signed by linear upsweep wavetrains. Time dithering was applied with the maximum random time shift of 0.256 s. This assumes a very difficult situation with a large number of sources, small separation of distance offsets and time shifts among shots in the blended-source array. For DSA-related scenarios, 3 types of frequency-banded and phased sources were used: the low frequency source of 1/4-12/20 Hz with 0 degree; the mid of 8/16-24/40 Hz with 120 degrees; the high of 16/32-48/96 Hz with 240 degrees. This was followed by deblended-data reconstruction of Ishiyama et al. (2018) using an iterative optimization scheme of sparse inversion, outputting the deblended data, $\langle \mathbf{P} \rangle$. Then, the both data, \mathbf{P} and $\langle \mathbf{P} \rangle$, were compared and evaluated based on the S/N, $\mathbf{P}/(\mathbf{P}-\langle \mathbf{P} \rangle)$.

Figure 2 shows an example of a conventional method. The sweep length is 18.5 s. Figures 2e and 2f show that the shot-generated wavefields are severely overlapped and interfered with each other even after the pseudo-deblending (i.e. after the adjoint of blending operation has been applied). In this scenario, it failed to achieve deblending. This is because the randomly scattered blended noise dominates and surpasses the blended signal; consequently, the iterative optimization scheme does not converge in stopping criteria in the sparse inversion algorithm.

Figure 3 shows an example of S-DSA. The shot-generated wavefields are frequency-banded and phased for each shot in the DSA array. The sweep length is 6.5 s each with its own sweep rate. Figures 3e and 3f show that pseudo-deblended are the designated and frequency-banded wavefields (the low frequency band for the 1st shot in this particular section), corresponding to filtering results naturally in the frequency domain. This allows straightforward deblending. The deblending problem is then switched to a data-reconstruction problem for spectrum recovery and balancing, corresponding to regularizing, interpolating data in each frequency band, and combining those as the full frequency band. This problem is solved by an iterative optimization scheme of sparse inversion. Figures 3g and 3h show that the temporal spectra

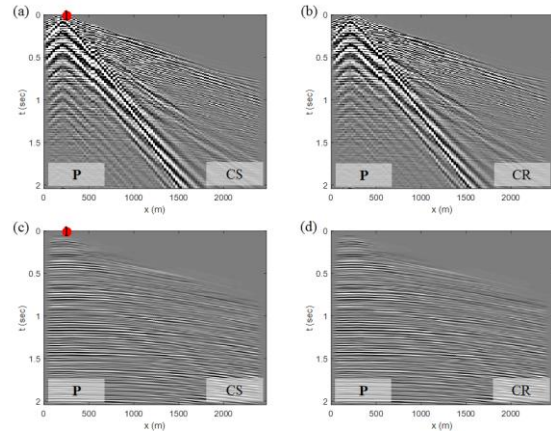


Figure 1. Reference data: (a) and (b) without noise attenuation; (c) and (d) with noise attenuation in the common-source (CS) and common-receiver (CR) domain, respectively. The red circle indicates the source and its shot location in this particular section.

were well recovered and balanced after iterations, and the deblended data were reasonably reconstructed with the S/N of 10 dB up.

Figure 4 shows a case of M-DSA. The shots are frequency-banded, phased and modulated, thereby so are the shot-generated wavefields. Following Takanashi et al. (2016), amplitude modulation is used for the modulating function. Such n signatures for n sources in the DSA array are encoded by repeating the original sweep wavetrain $l=2n-1$ times, followed by multiplying modulation carriers. The modulation carrier is a long-wavelength cosine function with its phase of $2\pi m_i \Delta f t$ ($m_i=0, 1, \dots, m$), where the integer $l < m < l/2$ is the number of modulation cycles, and Δf is the frequency sampling interval according to the total time length. The l -times repeated signature ($m_i=0$) is allocated in every l frequency samples, and the modulated signatures ($m_i=1, \dots, m$) are assigned at frequency channels $\pm m_i \Delta f$ from those of the repeated signature. The amplitudes of modulated signatures are halved due to the cosine effects. In this example, $n=5$, $l=9$ and $m=4$, thereby the sweep length is 58.5 s. Figures 4e and 4f show that pseudo-deblended are the demodulated, designated and frequency-banded wavefields, corresponding to results of filtering and physically separating frequency channels in the frequency domain. This allows simple and robust deblending. The wavefields are almost perfectly separated just after the pseudo-deblending. Again, the deblending problem is then switched to a data-reconstruction problem. Figures 4g and 4h show that the temporal spectra were entirely recovered and balanced after iterations, and the deblended data were successfully reconstructed with the S/N of 15 dB up.

Blended acquisition with S-M-DSA

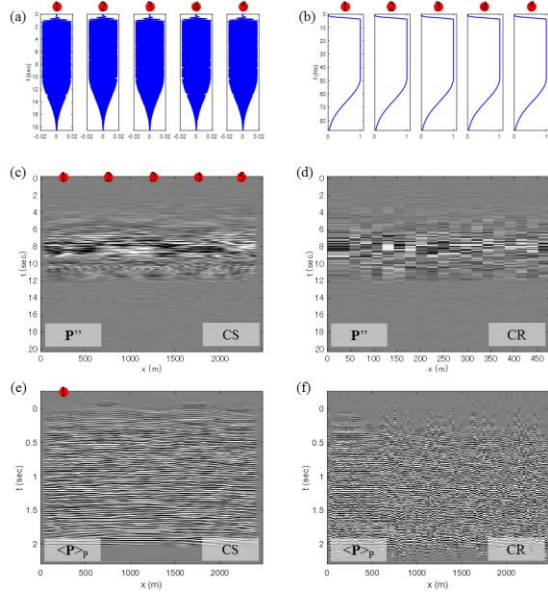


Figure 2. Example of a conventional method: (a) and (b) blending operators in the time and frequency domain for each shot in the blended-source array; (c) and (d) blended data; (e) and (f) pseudo-deblended data in the CS and CR domain, respectively. The red circles indicate the 5 sources and their shot locations in the blended-source array in this particular section.

Remember that the above examples use blended data numerically synthesized by the operators, thereby there is no difference between real signatures and preset reference ones in the operators. However, it is not a case in general for real blended data. Figure 5 shows the same case as Figure 4 except the operators containing random noise added to the reference signatures in the synthesizing process. This assumes a realistic situation. Furthermore, the blended data without noise attenuation were used. Figures 5g and 5h show that the deblended data were successfully reconstructed even in such realistic situations. This shows that the differences could be remedied by an iterative optimization scheme of sparse inversion during deblending.

Conclusively, our S-M-DSA method is suitable to fully achieve deblended-data reconstruction, thus totally and jointly achieve all shot-generated-wavefields separation, demodulation, designature, spectrum recovery and balancing, even in such difficult situations.

Discussions

The above examples reveal several benefits of our S-M-DSA method. First, our method requires only simple signaturing in the time dimension, since this method allows indeed straightforward deblending. This could even render any other blending properties unnecessary. Those, such as

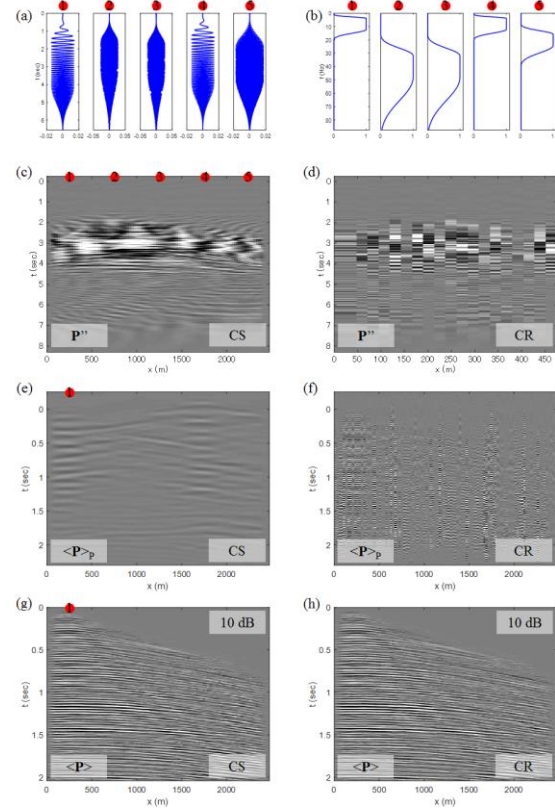


Figure 3. Example of S-DSA: (a) to (f) see Figure 2 caption; (g) and (h) deblended data with the SNR value after 100 iterations of deblended-data reconstruction in the CS and CR domain, respectively. See Figures 1c and 1d for comparison with the reference data. The 3 types of frequency-banded and phased sources are used: the low frequency source of 1/4-12/20 Hz with 0 degree; the mid of 8/16-24/40 Hz with 120 degrees; the high of 16/32-48/96 Hz with 240 degrees.

distance separation among shot locations and time shifts among shot times in the blended-source array, might not be required anymore. There might be no limitation on the number of sources in the blended-source array in order to secure successful deblending.

Second, our method allows non-uniform sampling and non-patterned shooting in the space dimension. This allows distributed, decentralized and dispersed source array, in which a swarm of the sources is independently, simultaneously and flexibly operational in a decentralized manner with no attempt to synchronize their activity.

Third, our method is feasible for vibrators that precisely control the sweep wavetrains on amplitudes, phases and frequencies. This is being available not only for land acquisition but also for marine because of the recent development of marine vibrators, thus even for transition

Blended acquisition with S-/M-DSA

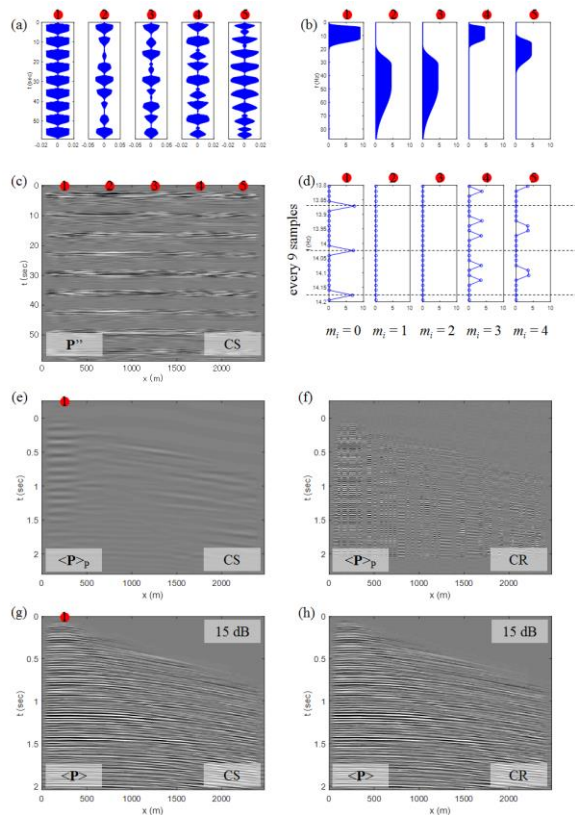


Figure 4. Example of M-DSA: (a) to (h) except (d) see Figure 3 caption; (d) zoomed-in plots of (b). See Figures 1c and 1d for comparison with the reference data. The repeated signature ($m_i=0$) is allocated in every 9 frequency samples, and the modulated signatures ($m_i=1, \dots, 4$) are assigned at frequency channels $\pm m_i \Delta f$ from those of the repeated one. The amplitudes of modulated signatures are halved.

zone using both land and marine vibrators. The deblending is sensitive to the accuracy of real signatures against preset reference ones. However, this method does not require complicated signaturing but relatively simple one. This might not cause severe differences. In addition, slight differences could be remedied by an iterative optimization scheme of sparse inversion during deblending as shown in the last example. Furthermore, some vibrator devices measure and record the actual motions including harmonics. The measurement could be used to enhance designature, thus the deblending performance.

Fourth, S-DSA can achieve higher acquisition productivity than conventional methods because of the shorter sweeping time. Besides, M-DSA should require repeating the original sweep wavetrain several times according to the number of sources ($l=2n-1$ times for n sources) for each shot in the DSA array. This might make the sweeping time per shot

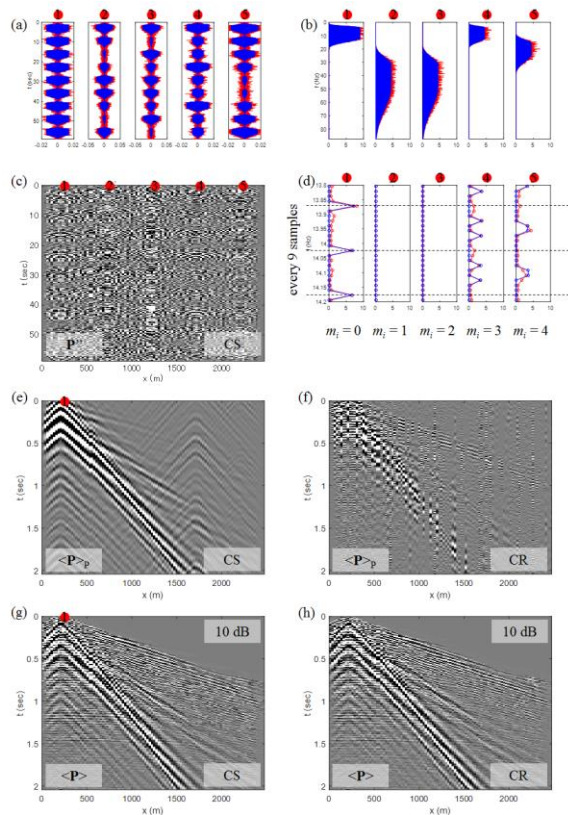


Figure 5. Example of M-DSA: (a) to (h) see Figure 4 caption. See Figures 1a and 1b for comparison with the reference data. Blending operators in blue indicate reference ones, and those with random noise in red assume real ones.

longer. However, M-DSA can still achieve higher productivity than traditional unblended acquisition. We will address this matter of interest by analyzing productivity on numbers of sources in the DSA array.

Conclusions

We introduced a blended-acquisition method, S-/M-DSA. The examples demonstrated that: S-DSA attains the best acquisition productivity with much less constraints in the encoding with more operational flexibility; M-DSA attains the best deblending performance, compared to other methods. Our method makes the blended-acquisition encoding and operations significantly simple and robust, as well as for the deblending processing.

Acknowledgements

We thank ADNOC and INPEX for their supports and permission to publish this paper.